

ZIF-9 with Enhanced Supercapacitor and Electrocatalytic for Oxygen Evolution Reaction Performances in Alkaline Electrolyte

Daojun Zhang¹, Jingchao Zhang^{1,*}, Helong Bai², Renchun Zhang¹, Huaizhong Shi¹, Baiqing Yuan^{1,*}

¹ Henan Province Key Laboratory of New Optoelectronic Functional Materials, College of Chemistry and Chemical Engineering, Anyang Normal University, Anyang 455002

² College of Chemistry, Jilin University, Changchun 130012

*E-mail: baqingyuan1981@126.com, zjc19830618@126.com

Received: 12 May 2016 / Accepted: 7 July 2016 / Published: 7 August 2016

Zeolitic imidazolate frameworks (ZIFs) are a new class of metal-organic materials built by tetrahedral metal ions and different imidazolate ligands. Own to the porous structure, exceptional thermal and chemical stability, ZIFs is considered to be promising candidates in various fields. In alkaline condition, the good catalytic activities of ZIF-9 for oxygen production were confirmed by its low overpotential, small tafel slope and high durability during oxygen evolution reaction. Furthermore, the cycling performance test of ZIF-9 shows that it can afford the highest capacitance after 3150 repeating cycles, then decreased slightly with furthermore charge–discharge cycles. The final specific capacitance of the ZIF-9 is 94.3% of its maximum value after 6000 cycles. These results show that ZIF-9 might be a capable electrode material for supercapacitor and water splitting electrocatalyst in the future.

Keywords: ZIF-9; Oxygen evolution reactions; Metal-organic frameworks; Supercapacitors; Electrocatalysts

1. INTRODUCTION

In recent twenty years, metal-organic frameworks (MOFs) have been widely researched to use in gas storage and separations, catalysis, fluorescent, sensors, nanomedicine, and imaging fields [1-6]. Nevertheless, the direct investigation of MOFs in the electrochemistry field is still in the initial stage, such as electrochemical sensors, lithium-ion batteries, supercapacitors, electrocatalysts in oxygen reduction reactions (ORR) and oxygen evolution reactions (OER) [7-16].

Over the last few years, various cobalt-based OER nanostructured structures have been designed for water oxidation catalysts [17-22]. Very recently, Mao et al. exhibited the first application of Cu-based MOF as electrocatalyst in ORR [16]. Wang reported Co-ZIF-9/FTO electrode as OER catalyst in a wide pH range [23]. A graphene–metalloporphyrin MOF composite with good catalytic activity for ORR and OER was also reported by Loh [24]. Because of most MOFs are fragile under basic condition and low conductivity, the research of MOFs as an independent OER electrocatalysts are rather rare. In addition, investigations into the exploitation of MOFs as supercapacitor electrode materials have attracted researchers' attention in recent years [25-31], however, the research in this field is still on an early stage and more challenging.

Zeolitic imidazolate frameworks (ZIFs) is a new kind of MOFs, which composed by imidazolate-based ligands and metal ions with a tetrahedral coordination mode. Generally, ZIFs show permanent porosity and exceptional thermal and chemical stability, thus ZIFs have been developed for direct use in many research fields. Nevertheless, to the best of our knowledge, there is only one report on the applications of MOFs as electrocatalyst for OER [17]. On the basis of the above considerations, herein, we reported ZIF-9 as supercapacitor electrode and OER electrocatalyst in alkaline electrolyte.

2. EXPERIMENTAL SECTION

2.1 Materials synthesis

Co(bIm)₂·(DMF)(H₂O) (ZIF-9) was synthesized following the reference [32] with slightly modified. A mixture of 105 mg Co(NO₃)₂·6H₂O (0.36 mmol), 30 mg benzimidazole (2.54 mmol), and 9.0 mL N, N'-dimethylformamide (DMF) was sealed in a 20 mL vial and kept at 130 °C for 48 h, and then naturally cooled down to 25 °C. Purple crystals were isolated and washed with DMF.

2.2 The characterization, preparation and measurement of supercapacitor electrode

X-ray diffraction (XRD) pattern of ZIF-9 was recorded on a Philips X'pert Pro X-ray diffractometer with Cu_{Kα} radiation ($\lambda=1.5418\text{\AA}$) and operated at 40 kV and 40 mA. A CHI 760E electrochemical analyzer system was used to fulfill all of the electrochemical measurements at room temperature. The electrochemical tests were performed in a three-electrode system with alkaline electrolyte solution, where a saturated calomel electrode (SCE) and a platinum foil were used as the reference and counter electrodes, respectively. The slurry of working electrode consisted of ZIF-9 active material, acetylene black and polyvinylidene fluoride with a weight ratio of 80:10:10, is blend by N-methyl-2-pyrrolidone. Then the slurry was pasted to the Ni foam (1 cm×1 cm) current collector and dried at 100 °C for 12 h under vacuum condition. Cyclic voltammetry (CV) and chronopotentiometry tests were conducted in 1 M KOH aqueous solution in the potential window of 0-0.46 V.

2.3 OER electrocatalytic electrode preparation and measurement

A solution mixed of water (700 μL), ethanol (250 μL) and Nafion (50 μL) containing 5 mg ZIF-9 powder were well blended under ultrasonic treatment to form a homogenous ink. Next, 5 μL of the catalyst ink was transferred to a polished glass carbon electrode with an area of 0.196 cm^2 and dried in air naturally. Platinum wire and Ag/AgCl were used as counter and reference electrodes, respectively. The electrolyte of 1 M KOH solution was puffed with bubbling O_2 for 30 min, and then the linear sweep voltametry (LSV) and Tafel curves were measured at 1600 rpm with a sweep rate of 1 mV/s with iR compensation enabled.

3. RESULTS AND DISCUSSION

The ZIF-9 was synthesized under the reported method by Yaghi et al. with a slightly modified [32]. The identity and purity of the compound was confirmed by the experimental X-ray powder diffraction (XRD) spectrum and showed in Fig.1.

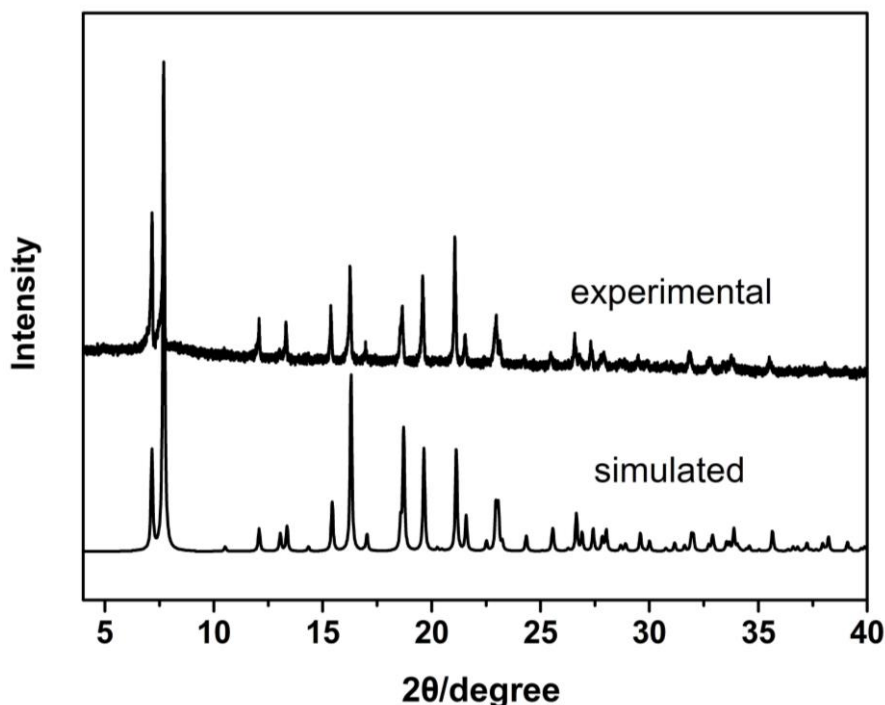


Figure 1. XRD patterns of the as-synthesized ZIF-9 sample and simulated.

XRD analyses revealed that the crystal structure of ZIF-9 was successfully synthesized, all peaks in experimental pattern consistent with the simulated XRD diffraction pattern of ZIF-9. In the structure of ZIF-9, cobalt ion is coordinated with four nitrogen atoms from four different benzimidazolate (bIm) ligands and each bIm ligand bridges two Co ions (Fig.2) and further forms a sodalite (SOD) topology framework (Fig. 3) [26].

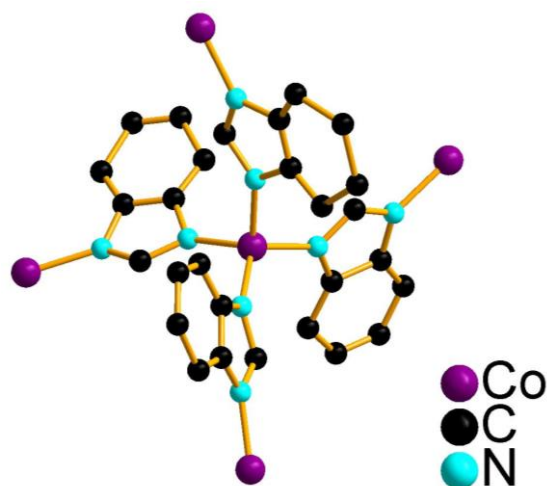


Figure 2. The tetrahedral coordination of benzimidazolone and cobalt ion.

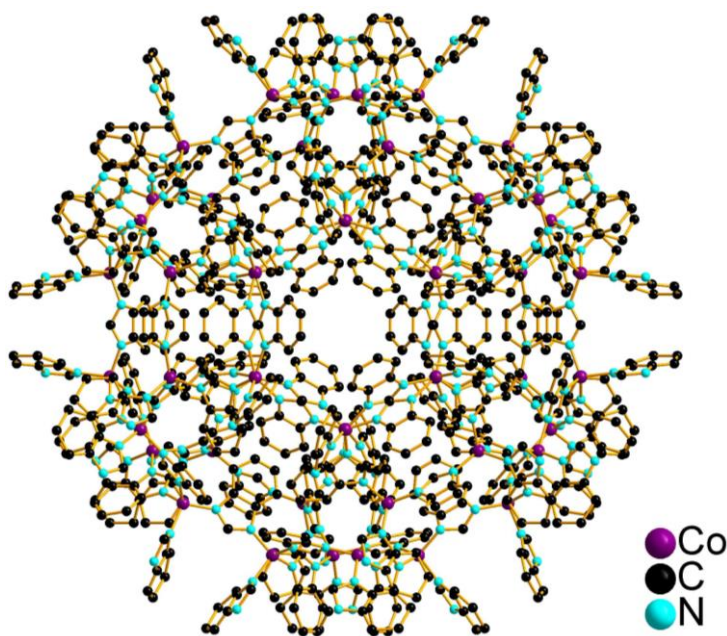


Figure 3. The 3D structure view of ZIF-9.

Fig.4a shows the CV experiments for ZIF-9 within a 0~0.50 voltage window at a scan rate from 5 to 50 mV s^{-1} . In each CV curve, we can observe a pair of redox peaks, which suggests the capacity of ZIF-9 is mainly attributed to the Faradaic redox reactions. At a low scan rate of 5 mV s^{-1} , the anodic and cathodic peaks located at 0.34 V and 0.15 V is ascribed to the redox process of $\text{Co}^{2+}/\text{Co}^{3+}$ redox couple, which achieve the electrical energy storage in the framework.

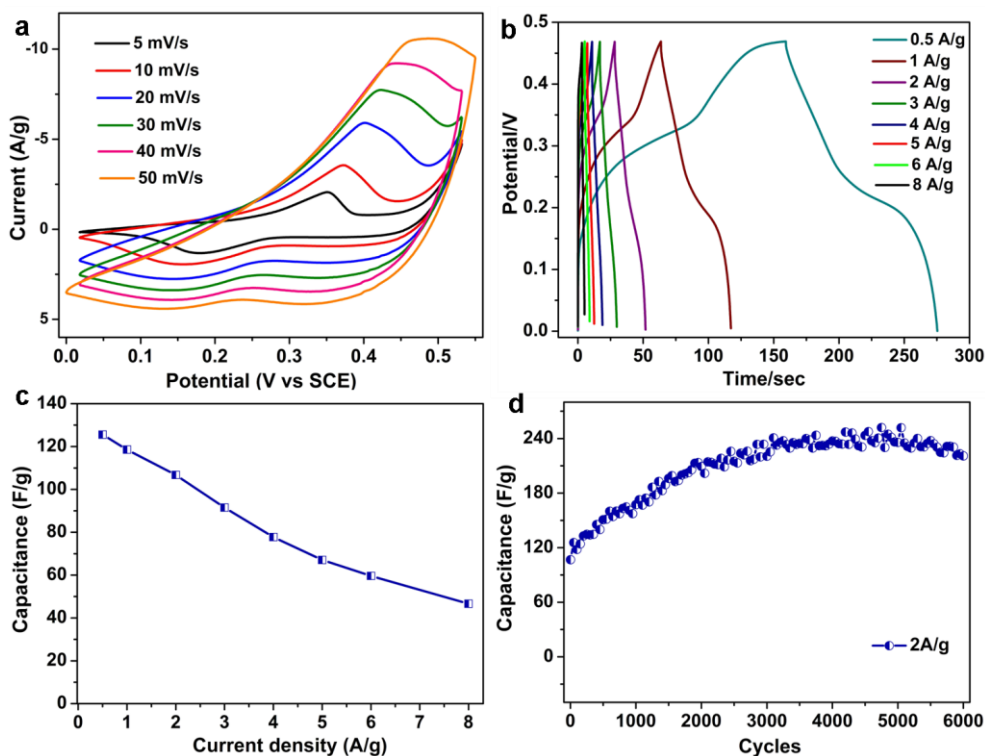


Figure 4. Supercapacitor electrochemical performance characterization: (a) CV curves of ZIF-9 electrode at various scan rates. (b) Galvanostatic charge-discharge curves of ZIF-9 at different current densities from 0.5 to 8 A g⁻¹. (c) The specific capacitances at different current densities of ZIF-9. (d) Cycling performance of ZIF-9 at a constant current density of 2 A g⁻¹.

ZIF-9 with high BET surface area and abundant porosity can provide more electroactive sites and channels for electrolyte ions diffusion, thus promote the ions migration and achieve high specific capacitances. The specific capacitance at various current densities is derived from the discharge curves and exhibited in Fig.4b. The ZIF-9 electrode material delivers specific capacitance of 125.5, 118.6, 106.7, 91.4, 77.7, 67.0, 59.6, and 46.6 F g⁻¹ at current densities of 0.5, 1, 2, 3, 4, 5, 6, and 8 A g⁻¹, respectively. In addition, the ZIF-9 sample maintains the highest capacitance of ~47.5 % as the current densities increasing from 0.5 to 6 A g⁻¹ (Fig.4c). The specific capacitances of ZIF-9 are compared to the reported mesoporous 437-MOF (81 F g⁻¹ at 1 A g⁻¹) [33], but lower than that of the supercapacitor electrodes of ZIF-67 microflowers (202.6 F g⁻¹ at 0.5 A g⁻¹) [34] and Ni-MOF-24 (1127 F g⁻¹ at 0.5 A g⁻¹) [35]. The cycling stability profile in Fig. 4d shows that the continuous charge-discharge cycles lead to the rising capacitance of ZIF-9, and the highest capacitance (240.7 at 2 A g⁻¹) was obtained at the 3150th cycles, then decreased slightly with furthermore charge-discharge cycles. The increasing capacitance along with the repeating cycles should be attributed to a time-consuming activation process of the porous ZIF-9. The final specific capacitance of the ZIF-9 is 94.3% of its maximum value after 6000 cycles. The results demonstrate that ZIF-9 might be a probable material for high-performance supercapacitor in future.

To investigate the OER electrocatalytic performance of ZIF-9, the test was conducted in a three electrode setup in a 1 M KOH alkaline solution under a rotating rate of 1600 rpm to send out the

generated O₂. The CV and LSV curves of ZIF-9 is probed at a scan rate of 1 mV s⁻¹ (Fig. 5a and b), the ZIF-9 electrode present a dramatic increase of polarized current at ~1.5 V versus reversible hydrogen electrode (RHE) and the overpotential of ZIF-9 electrode was 1.592 V versus E_{RHE} ($\eta=362$ mV) to delivering 10 mA/cm² current density, suggesting its high activity of the ZIF-9 for OER (Fig. 5b). The OER catalytic kinetics was further studied using Tafel plot derived from the LSV. The linear region was fitted to the Tafel equation ($\eta = b \log j + a$), the ZIF-9 exhibits a Tafel slope of 68.35 mVdec⁻¹ (Fig. 5c), which is comparable to the typical cobalt oxide OER electrocatalyst[36]. The relative small Tafel slope and high current density of the ZIF-9 might be ascribed to the fast charge transport kinetics of the porous framework. In addition, the exposure of the surface Co atoms in ZIF-9 structure may be essential to the electrochemical oxygen evolution process. The stability test for the ZIF-9 was carried out by continuously performing the OER on a modified RDE in a 1 M KOH alkaline solution. Galvanostatic curve for ZIF-9 was measured for over 7200 s, only a slight increase of the potential (~11 mV) for ZIF-9 was observed. Low overpotential, high catalytic current and relatively small Tafel slope indicate that ZIF-9 is potential non-precious metal OER electrocatalyst.

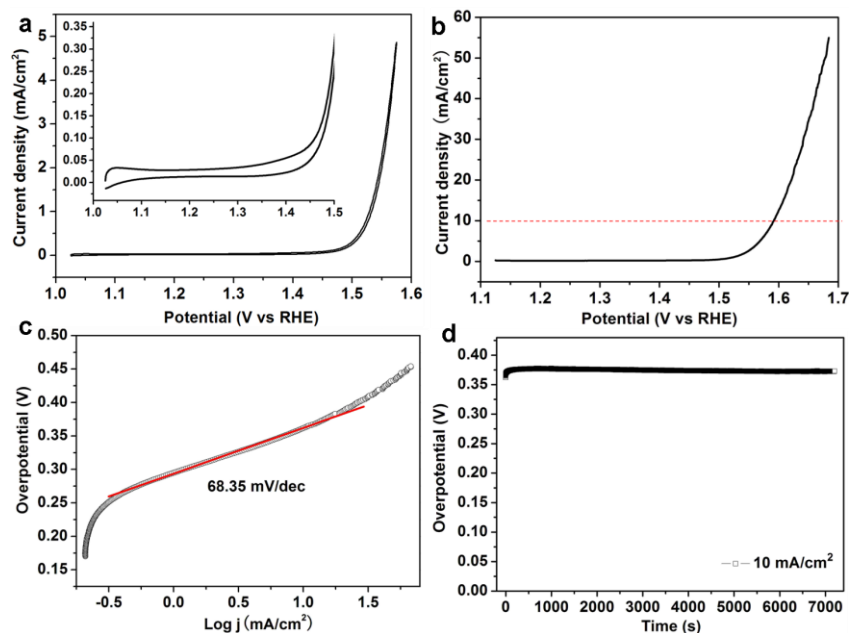


Figure 5. OER electrochemical performance characterization at a continuous electrode rotating speed of 1600 rpm in 1 mol L⁻¹ KOH: (a) Cyclic voltammograms of the ZIF-9 obtained at 1 mVs⁻¹, inset is a amplification of CV curve at the potential of 1.0~1.5 V (vs RHE). (b) Polarization curves of ZIF-9 catalysts at a scan rate of 1 mVs⁻¹ with iR compensation enabled. (c) Tafel plots of OER currents derived from (b). (d) Chronopotentiometry curves of ZIF-9 on a glassy-carbon RDE at a constant current density of 10 mA cm⁻² for 7200 s.

4. CONCLUSIONS

In summary, the OER activity evaluation demonstrated the ZIF-9 is attractive as an electrode material used alone for water electrolysis catalyst. Furthermore, it can deliver a catalytic current

density of 10 mA cm^{-2} at a low overpotential of 0.362 V and a favorable OER kinetic with a small Tafel slope of 68.35 mV/dec. In addition, ZIF-9 may be a good candidate of electrochemical capacitor with a high specific capacitance up to 118.6 F g^{-1} at a current density of 1 A g^{-1} and the final specific capacitance of the ZIF-9 keeps 94.3% of its maximum value after 6000 cycles at a current density of 2 A g^{-1} . It is anticipated that the ZIF-9 may be a desirable electrochemical electrode material for practical applications.

ACKNOWLEDGMENTS

Financial supports from the National Science Foundation of China (Nos. 21501006, 21405005, U1404208, 21301009), Scientific Research Foundation for the Returned Overseas Chinese Scholars, State Education Ministry, and Foundation of Henan Educational Committee (No. 15A150002, 15A150031, 13B150893) are gratefully acknowledged.

References

1. R. J. Kuppler, D. J. Timmons, Q. R. Fang, J. R. Li, T. A. Makal, M. D. Young, D. Q. Yuan, D. Zhao, W. J. Zhuang and H. C. Zhou, *Coord. Chem. Rev.*, 253 (2009) 3042.
2. Y. J. Cui, Y. F. Yue, G. D. Qian and B. L. Chen, *Chem. Rev.*, 112 (2012) 1126.
3. P. Ramaswamy, N. E. Wong and G. K. H. Shimizu, *Chem. Soc. Rev.*, 43 (2014) 5913.
4. A. H. Chughtai, N. Ahmad, H. A. Younus, A. Laypkovc and F. Verpoort, *Chem. Soc. Rev.*, 44 (2015) 6804.
5. H. Furukawa, K. E. Cordova, M. O'Keeffe and O. M. Yaghi, *Science*, 341 (2013) 974.
6. C. B. He, D. M. Liu and W. B. Lin, *Chem. Rev.*, 115 (2015) 11079.
7. S. L. Li and Q. Xu, *Energy Environ. Sci.*, 6 (2013) 1656.
8. D. F. Wu, Z. Y. Guo, X. B. Yin, Q. Q. Pang, B. B. Tu, L. J. Zhang, Y. G. Wang and Q. W. Li, *Adv. Mater.*, 26 (2014) 3258.
9. F. X. Yin, G. R. Li and H. Wang, *Catal. Commun.*, 54 (2014) 17.
10. J. S. Li, S. L. Li, Y. J. Tang, M. Han, Z. H. Dai, J. C. Bao and Y. Q. Lan, *Chem. Commun.*, 51 (2015) 2710.
11. Y. Gong, H. F. Shi, P. G. Jiang, W. Hua and J. H. Lin, *Cryst. Growth Des.*, 14 (2014) 649.
12. Y. P. Liu, S. X. Guo, A. M. Bond, J. Zhang and S. W. Du, *Electrochimica Acta*, 101 (2013) 201.
13. M. Jiang, L. J. Li, D. D. Zhu, H. Y. Zhang and X. B. Zhao, *J. Mater. Chem. A*, 2 (2014) 5323.
14. J. S. Li, Y. Y. Chen, Y. J. Tang, S. L. Li, H. Q. Dong, K. Li, M. Han, Y. Q. Lan, J. C. Bao and Z. H. Dai, *J. Mater. Chem. A*, 2 (2014) 6316.
15. M. Jahan, Q. L. Bao and K. P. Loh, *J. Am. Chem. Soc.*, 134 (2012) 6707.
16. J. J. Mao, L. F. Yang, P. Yu, X. W. Wei and L. Q. Mao, *Electrochem. Commun.*, 19 (2012) 29.
17. G. S. Hutchings, Y. Zhang, J. Li, B. T. Yonemoto, X. G. Zhou, K. K. Zhu and F. Jiao, *J. Am. Chem. Soc.*, 137 (2015) 4223.
18. H. Y. Jin, J. Wang, D. F. Su, Z. Z. Wei, Z. F. Pang and Y. Wang, *J. Am. Chem. Soc.*, 137 (2015) 2688.
19. Y. W. Liu, H. Cheng, M. J. Lyu, S. J. Fan, Q. H. Liu, W. S. Zhang, Y. D. Zhi, C. M. Wang, C. Xiao, S. Q. Wei, B. J. Ye and Y. Xie, *J. Am. Chem. Soc.*, 136 (2014) 15670.
20. T. Y. Ma, S. Dai, M. Jaroniec and S. Z. Qiao, *J. Am. Chem. Soc.*, 136 (2014) 13925.
21. L. Xu, Q. Q. Jiang, Z. H. Xiao, X. Y. Li, J. Huo, S. Y. Wang and L. M. Dai, *Angew. Chem. Int. Ed.*, 55 (2016) 5277.
22. M. R. Gao, Y. F. Xu, J. Jiang, Y. R. Zheng and S. H. Yu, *J. Am. Chem. Soc.*, 134 (2012) 2930.
23. S. B. Wang, Y. D. Hou, S. Lin and X. C. Wang, *Nanoscale*, 6 (2014) 9930.
24. M. Jahan, Z. L. Liu and K. P. Loh, *Adv. Funct. Mater.*, 23 (2013) 5363.

25. R. Díaz, M. G. Orcajo, J. A. Botas, G. Calleja and J. Palma, *Mater. Lett.*, 68 (2012) 126.
26. D. Y. Lee, S. J. Yoon, N. K. Shrestha, S. H. Lee, H. Ahn and S. H. Han, *Micropor. Mesopor. Mater.*, 153 (2012) 163.
27. D. Y. Lee, D. V. Shinde, E. K. Kim, W. Lee, I.-W. Oh, N. K. Shrestha, J. K. Lee and S. H. Han, *Micropor. Mesopor. Mater.*, 171 (2013) 53.
28. Y. Gong, J. Li, P. G. Jiang, Q. F. Li and J. H. Lin, *Dalton Trans.*, 42 (2013) 1603.
29. K. M. Choi, H. M. Jeong, J. H. Park, Y. B. Zhang, J. K. Kang and O. M. Yaghi, *Acs Nano*, 8 (2014) 7451.
30. J. Yang, C. Zheng, P. X. Xiong, Y. F. Li and M. D. Wei, *J. Mater. Chem. A*, 2 (2014) 19005.
31. A. Borenstein, O. Fleker, S. Luski, L. Benisvy and D. Aurbach, *J. Mater. Chem. A*, 2 (2014) 18132.
32. K. S. Park, Z. Ni, A. P. Côté, J. Y. Choi, R. D. Huang, F. J. Uribe-Romo, H. K. Chae, M. O’Keeffe and O. M. Yaghi, *PNAS*, 103 (2006)10186.
33. M. Du, M. Chen, X. G. Yang, J. Wen, X. Wang, S. M. Fang and C. S. Liu, *J. Mater. Chem. A*, 2 (2014) 9828.
34. D. J. Zhang, H. Z. Shi, R. C. Zhang, Z. R. Zhang, N. Wang, J. W. Li, B. Q. Yuan, H. L. Bai and J. C. Zhang, *RSC Adv.*, 5 (2015) 58772.
35. J. Yang, P. X. Xiong, C. Zheng, H. Y. Qiu and M. D. Wei, *J. Mater. Chem. A*, 2 (2014) 16640.
36. Z. Q. Jiang, Z. J. Jiang, T. Maiyalagan and A. Manthiram, *J. Mater. Chem. A*, 4 (2016) 5877.

© 2016 The Authors. Published by ESG (www.electrochemsci.org). This article is an open access article distributed under the terms and conditions of the Creative Commons Attribution license (<http://creativecommons.org/licenses/by/4.0/>).